International Journal of Bifurcation and Chaos, Vol. 9, No. 10 (1999) 2081–2090

STABILITY OF ORDER: AN EXAMPLE OF HORSESHOES "NEAR" A LINEAR MAP

ERIK M. BOLLT*
Department of Mathematics, 572 Holloway Rd., U.S. Naval Academy, Annapolis, MD 21402-5002, USA

Received October 16, 1998; Revised March 12, 1999

We have been motivated by a question of "anticontrol" of chaos [Schiff *et al.*, 1994], in which recent examples [Chen & Lai, 1997] of controlling nonchaotic maps to chaos have required large perturbations. Can this be done without such brute force? In this paper, we present an example in which a family of maps, G_ε, numerically displays a transverse homoclinic point, and hence a horseshoe and chaos, for a fixed value of the parameter ε. We show that these maps converge pointwise to a linear map. Furthermore, a simple scaling conjugacy is shown for a family of maps which even shows geometric similarity of all relevant structures. This is in seeming contradiction to well-known structural stability results concerning horseshoes, but careful consideration reveals that these theorems require convergence in a uniform topology in function space. We show that no such convergence is possible for our family of maps, since it is impossible to find a finite radius disk which contains all of the horseshoes Λ_ε for every ε. Thus, there is no contradiction. Our example may be considered to be a new kind of bifurcation route to chaos by horseshoes, in which rather than creating/destroying a horseshoe by creating/destroying transverse homoclinic points, the horseshoe is sent/brought to/from infinity.

1. Introduction

In this paper, we address the question of how "far" from an obviously simple dynamical system might one find a chaotic dynamical system. We have chosen an example family of continuously ε-parameterized maps G_ε, for which G_0 is linear, but f_ε is chaotic for any $\varepsilon > 0$.

Our motivation in this question is to investigate possible "fine-tuning" in a control mechanism which might drive a simple (linear) system to chaos. Such control, from order to chaos, has been characterized as "anticontrol," of chaos [Schiff *et al.*, 1994]. Controlling chaos has been a hot topic in the dynamical systems literature [Ott *et al.*, 1990; Chen & Dong, 1998; Kapitaniak, 1996], since controls which explicitly exploit chaos offer rich flexibility and agility [Shinbrot *et al.*, 1993; Kostelich *et al.*, 1993; Bollt & Meiss, 1995; Schweizer & Kennedy, 1995; Bollt & Kostelich, 1998]. In particular, chaos is often a beneficial property which anticontrol strives to exploit even if the process was not originally chaotic. For example, chaos is helpful for fluid mixing [Ottino, 1989] by "chaotic advection," and to cite a biological example, chaos is now thought to be necessary in the (human) brain [Schiff *et al.*, 1994].

In recent work [Chen & Lai, 1997], the authors showed that a rather arbitrary nonlinear dynamical system,

$$\mathbf{x}_{n+1} = \mathbf{f}(\mathbf{x}_n)\,, \tag{1}$$

with $\mathbf{f} \in C^1(\Re^n)$, may be anticontrolled by a combination of linear state-feedback and a mod operation to yield a rigorously chaotic process.

*E-mail: bollt@nadn.navy.mil

That is, a feedback input sequence $\{\mathbf{u}_k\}_{k=0}^{\infty}$,

$$\mathbf{x}_{n+1} = \mathbf{f}(\mathbf{x}_n) + \mathbf{u}_n \,, \tag{2}$$

is used to effectively generate a process with positive Luyapunov exponent(s), which we characterize in 1-D by the linear map $f(x)$,

$$x_{n+1} = f(x) = 2x_n \,, \tag{3}$$

with exponent $\lambda = \ln 2$, defining the stretching component of chaos. Further introducing a mod(1) operation,

$$x_{n+1} = g(x) = 2x_n \bmod(1) \,, \tag{4}$$

effectively introduces a second ingredient for chaos, folding and continual refolding. In fact, Eq. (4) can easily be shown [Ott, 1994] to be topologically (semi)conjugate[1] to the Bernoulli shift map on two symbols, which in turn can be shown to be rigorously chaotic according to the well-accepted definition of Devaney [1989], requiring (1) sensitive dependence on initial conditions, (2) topological transitivity, (3) a dense set of periodic orbits. In fact, conditions (1) and (2) are sufficient, as (3) follows [Martelli *et al.*, 1998]. But $f(x)$ and $g(x)$ from Eqs. (3) and (4) are quite "far" from each other, say in an L^2 sense; this sufficient anticontrol is brutish. Is such brute force necessary? Therefore, the "fine-tuning" part of our question is: *Given a linear dynamical system $f(x)$, can a nearby dynamical system $g(x)$ be found which is chaotic.* In this paper, we explicitly construct such an example.

If we wish to find a $g(x)$ with a horseshoe, the converse of structural stability theorems (see Theorem 1) indicate that no such $g(x)$ may exist "nearby" $f(x)$. In brief, structural stability of horseshoes imply that in a "neighborhood" of a $g(x)$, which has a horseshoe, all "nearby" maps $g(x)+\delta g(x)$ also have topologically conjugate horseshoes. This is in seeming contrast to the example which we explicitly construct here. The loophole which allows our example is in the topology. We have thus far been deliberately vague in defining the topology in which we measure function distance, as this is exactly the sensitive issue on which our question and discussion pivots. It turns out that structural stability results we refer to rely on the uniform topology, and the example we present in this paper is a family of maps which converge pointwise to a linear map, but for each nonzero perturbation displays a horseshoe; our sequence of maps does not converge uniformly to the linear map, in agreement with the requirement that such is forbidden by the converse structural stability theorems.

2. Structural Stability

In the guise of a control problem, we have restated the question of "structural stability" [Hirsch & Smale, 1974]. In particular, Smale was interested in topologically significant behavior, in the sense that their behavior could not be simply "perturbed-away" by small noise or modeling errors. Therefore, structurally stable properties could be considered to be physically relevant, since they would not disappear in the unavoidable presence of small noise. Devaney introduces [Devaney, 1989], "Briefly, a map f is structurally stable if every 'nearby' map is topologically conjugate to f and so has essentially the same dynamics," but he goes on to point-out the importance of a precise meaning for the word "nearby."

The C^r topology[2] is commonly used to define structural stability.

Definition 1 [Katok & Hasselblatt, 1995]. A C^r map $f : M \to M$ is C^m-structurally stable, $1 \le m \le r$, if there exists a C^m topological

[1]Two maps $f : M \to M$ and $g : N \to N$ are *topologically conjugate* if there exists a homeomorphism $h : M \to N$ which commutes, $f = h^{-1} \circ g \circ h$, and we write $f \sim g$ [Katok & Hasselblatt, 1995]. If h is only a surjection, then we say there is a semi-conjugacy.

[2]The C^r topology is easily defined for 1-D functions. Given two functions $f, g : M \to M$, and $M \subseteq \Re$, the $C^0(M)$ topology follows the C^0-metric: $\rho_{C^0(M)}(f, g) = \sup_{x\in M} |f(x) - g(x)|$. Similiarly, the C^r-metric, $\rho_{C^r(M)}(f, g) = \sup_{x\in M}(|f(x) - g(x)|, \ldots, |f^{(r)}(x) - g^{(r)}(x)|$, defines the associated $C^r(M)$ topology. Note that $\rho_{C^r(M)}(f, g)$ is a well-defined metric only for a compact $M \not\subseteq \Re$, e.g. an interval. The natural extension to transformations in $\Re^n$, for compact metrizable topological spaces, such as a compact manifold M, follows the C^0 or *uniform* topology, again following $\rho_{C^0(M)}(f, g) = \sup_{\mathbf{x}\in M} |f(\mathbf{x}) - g(\mathbf{x})|$. Then, the C^1 topology follows the C^0 topology. Given f, g and Jacobian derivatives Df and Dg, $\rho_{C^1(M)}(f, g) = \max(\rho_{C^1(M)}(f, g), \|Df - Dg\|_0)$ and $\|Df - Dg\|_0 = \sup_{\mathbf{v}\in TM,\, \|v\|=1}(Df - Dg)\cdot\mathbf{v}$ denotes the sup-norm on the tangent space. Likewise, there is an extension to $C^r(M)$ [Katok & Hasselblatt, 1995]. Our main point is the importance of a compact domain to the issue of "nearby" in the definition of structural stability.

neighborhood U of f, such that every $g \in U$ is topologically conjugate, $f \sim g$.

It turns out that for this definition to make sense, we must be careful to choose a metrizable domain M, such as a compact manifold. Note that on an unbounded domain, two seemingly nearby functions are infinitely C^r-apart (see footnote 1). For example, let $f(x) = 2x$, and $g(x) = (2 + \varepsilon)x$, then $\rho_{C^r(\Re)}(f, g) = \sup_{x\in\Re}(|f(x) - g(x)|, \ldots, |f^{(r)}(x) - g^{(r)}(x)| = \infty$, for every $\varepsilon > 0$, even while they are considered C^r-close when measured on a compact domain, such as $M = [a, b]$ is an interval, $\rho_{C^0([a,b])}(f, g) = \sup_{x\in[a,b]} |f(x) - g(x)| = \max(2|a|\varepsilon, 2|b|\varepsilon)$. For 1-D maps, a specialization of Definition 1 can be found in [Devaney, 1989], by requiring $M = [a, b]$ is an interval, and therefore a $C^r(M)$ ε-neighborhood of f, or *ball*, may be denoted $B_\varepsilon^{C^r(M)}(f)$, $\varepsilon > 0$, consists of $B_\varepsilon^{C^r(M)}(f) = \{g \in C^r(M) : \rho_{C^r(M)}(f, g) < \varepsilon\}$, and these balls generate arbitrary neighborhoods U.

We will present a model in the next section, which we argue has horseshoes for every nonzero value of the parameter, but the model is arbitrarily close to a linear map. This is seemingly in conflict with the following theorem, but that the example is allowed to exist is realized by careful consideration of the metric with which we measure "nearby" in function space.

Theorem 1 [Katok & Hasselblatt, 1995]. *Given a C^1 diffeomorphism $f : U \to M$, with the maximal invariant set Λ of the horseshoe of f, then any g sufficiently C^1 close to f has an invariant set Λ' such that $f|_\Lambda$ is conjugate to $f'|_{\Lambda'}$: there exists a homeomorphism $h : \Lambda \to \Lambda'$ such that $h \circ f|_\Lambda = f'|_{\Lambda'} \circ h$*

3. From a Linear Model to Horseshoes

We begin with an obviously simple and nonchaotic dynamical system, the linear equation,

$$\mathbf{x}_{n+1} = L(\mathbf{x}_n) = A \cdot \mathbf{x}_n \,, \tag{5}$$

where for simplicity's sake, we choose $x_n \in \Re^2$. Therefore, our goal is to design a dynamical system $\mathbf{x}_{n+1} = \mathbf{f}(\mathbf{x}_n)$, which is chaotic and arbitrarily close to Eq. (5). To further simplify a concrete problem, for now we assume a hyperbolic saddle in orthogonal coordinates,

$$A = \begin{pmatrix} c & 0 \\ 0 & d \end{pmatrix} , \quad d > 1 \,, \quad 0 < c < 1 \,. \tag{6}$$

With stable manifold $W^s(0) = E^s(0) = \{(x, y) : y = 0\}$, and unstable manifold $W^u(0) = E^u(0) = \{(x, y) : x = 0\}$. We choose,

$$c = \frac{1}{2} \,, \quad \text{and} \quad d = 2 \,, \tag{7}$$

in the rest of the following. We thus begin with the "stretch" ingredient already in place, but we discuss control to such point from arbitrary starting points in the conclusion section. First we strive to design a perturbation of the linear map to introduce the "fold" ingredient of chaos.

We recall [Smale, 1963; Wiggins, 1992; Katok & Hasselblatt, 1995] the famous "horseshoe" theorem due to Smale, on which motivation for our construction relies.

Theorem 2 [Smale, 1963; Wiggins, 1992; Katok & Hasselblatt, 1995]. *Given a C^r diffeomorphism f, $r \geq 2$, with hyperbolic periodic point $\mathbf{p}$, such that $W^s(\mathbf{p})$ and $W^u(\mathbf{p})$ intersect transversally, then there exists integer time $n \geq 1$ such that f^n has an invariant Cantor set, Λ. Furthermore, there exists a conjugacy $h : \Lambda \to \Sigma_2$ such that $h \circ f^n|_\Lambda = s \circ h$, where Σ_2 is the full 2-shift, and s is the Bernoulli shift map.*

Hence, our goal is to fold the unstable manifold of Eq. (5) onto the stable manifold; the resulting dynamical system has a homoclinic point, possibly transverse, and hence, an embedded horseshoe. Furthermore, our goal is to achieve the horseshoe with a (suitably defined) small perturbation to the map. As already mentioned when stating structural stability Theorem 1, these are conflicting goals; the existence of the following solution, which we now construct, is permitted by carefully considering how "close" is defined.

To control the variation from the linear model Eq. (5), we design an ε-parameterized family of dynamical systems,

$$G_\varepsilon = F_\varepsilon \circ L \,, \tag{8}$$

such that,

$$F_0 = I \,, \tag{9}$$

is the identity transformation when $\varepsilon = 0$, but G_ε is chaotic for every $\varepsilon > 0$.

4. Rotation to Fold

We have chosen a rotation model, to achieve the desired folding. Let,

$$F_\varepsilon(\mathbf{z}) = \begin{pmatrix} r\,\cos(\theta + \varepsilon r^\alpha) \\ r\,\sin(\theta + \varepsilon r^\alpha) \end{pmatrix}, \tag{10}$$

where,

$$r = \sqrt{x^2 + y^2}, \quad \theta = \tan^{-1}\left(\frac{y}{x}\right). \tag{11}$$

We find that if $\alpha = 0$, then F_ε does not rotate the unstable manifold of $G_\varepsilon = F_\varepsilon \circ L$, $W^u_{G_\varepsilon}(\mathbf{z})$ fast enough to overcome the exponential growth along the unstable manifold of L. However, we observe that $\alpha \geq 1$ is sufficient, and we choose $\alpha = 1$ in what follows.

We see that $F_\varepsilon(\mathbf{z})$ is continuously differentiable for all $\mathbf{z} \neq 0$, and the discontinuity is removable. So we let $F_\varepsilon(\mathbf{0}) = L(\mathbf{0})$. Therefore, we have an inverse of the map, $G_\varepsilon^{-1} = L^{-1} \circ F_\varepsilon^{-1}$, where F_ε^{-1} and L^{-1} are each easily computed.

In Figs. 1 and 2, we show the evolution of a unit circle, under repeated iterations of G_ε and G_ε^{-1}, for fixed $\varepsilon = 1/100$. These figures give numerical evidence that under several iterations, the unit circle folds completely back over itself in a manner which suggest an embedded horseshoe Λ_ε. In fact, the double folding of the unit circle over itself suggests the existence of a larger embedded set Υ_ε which is conjugate to the full 3-shift Σ_3. We use the subscript "ε" to index the sets Λ_ε and Υ_ε, because the scaling conjugacy presented in the next section means that the existence of such sets for any one ε forces a corresponding set for all $\varepsilon > 0$.

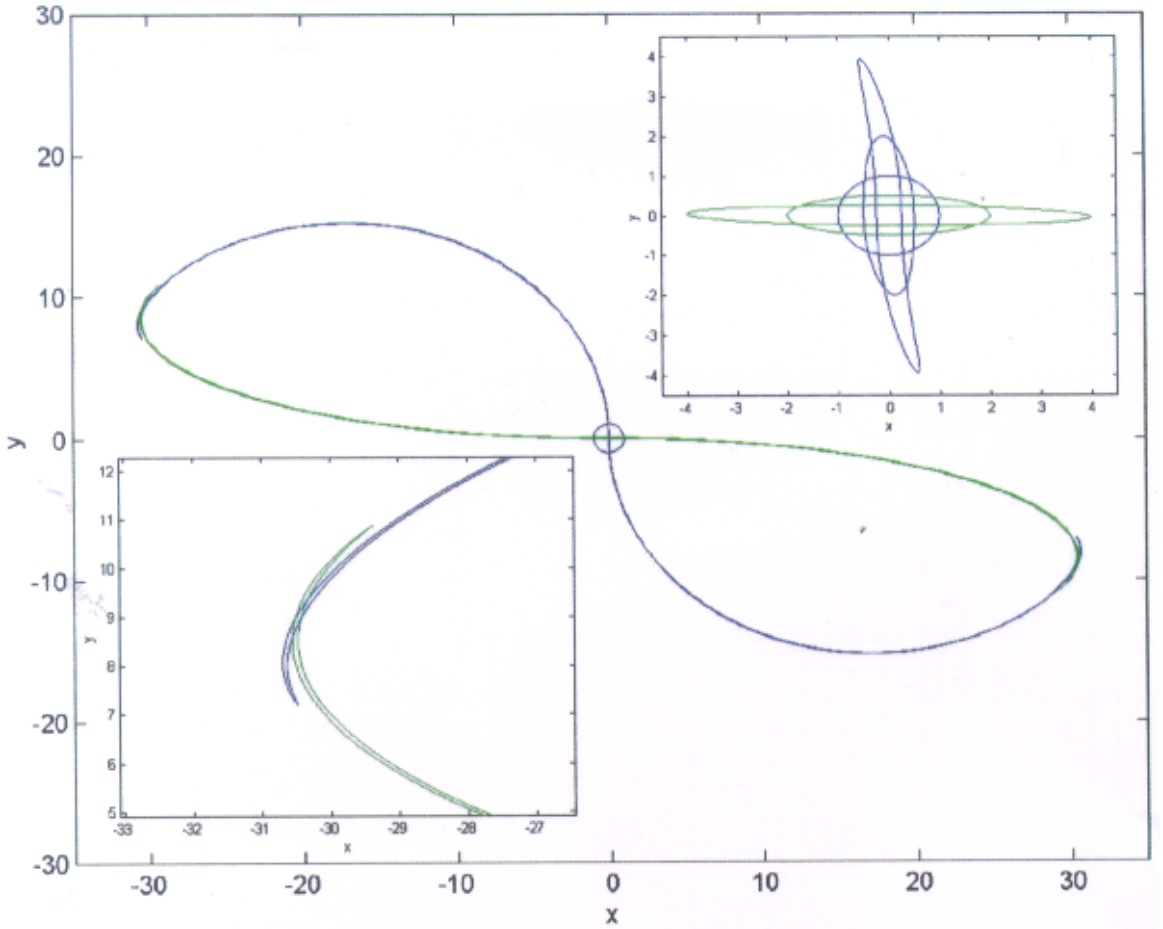

Fig. 1. Evolution of a unit circle under repeated iterations by the map G_ε, $\varepsilon = 1/100$. Upper-right inset: The unit circle S, and the (pre)iterates $G_\varepsilon^{-2}(S)$, $G_\varepsilon^{-1}(S)$, $G_\varepsilon(S)$, and $G_\varepsilon^2(S)$. Lower-left inset and center: We see that $G_\varepsilon^{-6}(S)$ intersects $G_\varepsilon^6(S)$ transversally in a manner indicating a horseshoe (see Fig. 2). For other values of ε, we get the same kind of "overlap" intersection between $G_\varepsilon^{-m}(S)$ intersects $G_\varepsilon^m(S)$, for some $m(\varepsilon)$.

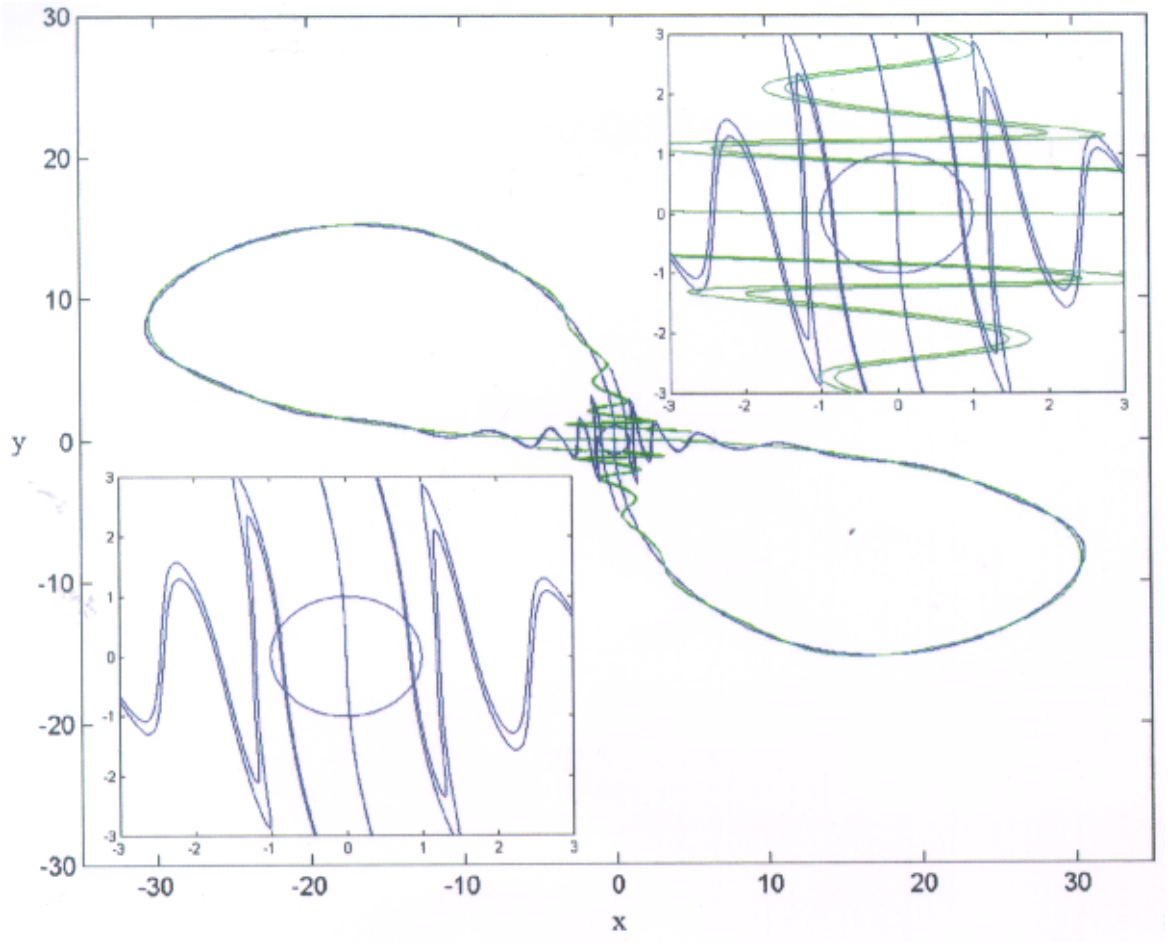

Fig. 2. A unit circle S the 12th (pre)iterate under the map G_ε^{12}, G_ε^{-12}, $\varepsilon = 1/100$. Lower-left inset: G_ε^{12} folds completely across S, numerically indicating a horseshoe, and the double folding across S indicates a conjugacy to the 3-shift Σ_3. Upper-right inset: The developing tangle of G_ε^{12}, G_ε^{-12} over S.

Consider implications of slowly decreasing ε toward zero.

Remark 1. By continuity of F_ε with respect to ε, we have the pointwise convergence, $G_\varepsilon(\mathbf{z}) \to L(\mathbf{z})$ as $\varepsilon \to 0^+$, for each $\mathbf{z}$. Thus, small controls ε give small $\|G_\varepsilon(\mathbf{z}) - L(\mathbf{z})\|_2$, for each fixed $\mathbf{z}$.

Remark 2. Numerical observations in Figs. 1–3 indicate that $G_\varepsilon(\mathbf{z})$ has a transverse homoclinic point, and hence a horseshoe for every positive ε. We will give more rigorous support to these numerical observations in the next section.

In Figs. 4 and 5, we numerically show the consequences of decreasing ε. In short, the homoclinic tangles are geometrically similar for all $\varepsilon > 0$. We give rigorous proof of this in the next section. Therefore, each homoclinic point moves along a line-ray emanating from the origin as ε is decreased toward zero, which is seen in Fig. 4, where several primary homoclinic points are highlighted (circled) for a sequence of ε_i, with lines drawn connecting each correspondingly moved intersection points. Geometric similarity also implies that the angles between stable and unstable manifolds at each homoclinic point must be preserved, which is what we observe in Fig. 5. Thus, when ε is adjusted, we do not expect any angles between stable and unstable manifolds to deform to nontransversality, as is a traditional bifurcation route for the destruction of a horseshoe.

That a horseshoe map can be found arbitrarily close to a linear map is seemingly in conflict with the well-known result that horseshoes are structurally stable. In light of Theorem 1, Remark 2 seems impossible, since maps "nearby" maps with horseshoes must also have horseshoes, but the "loophole" is in the definition of nearby.

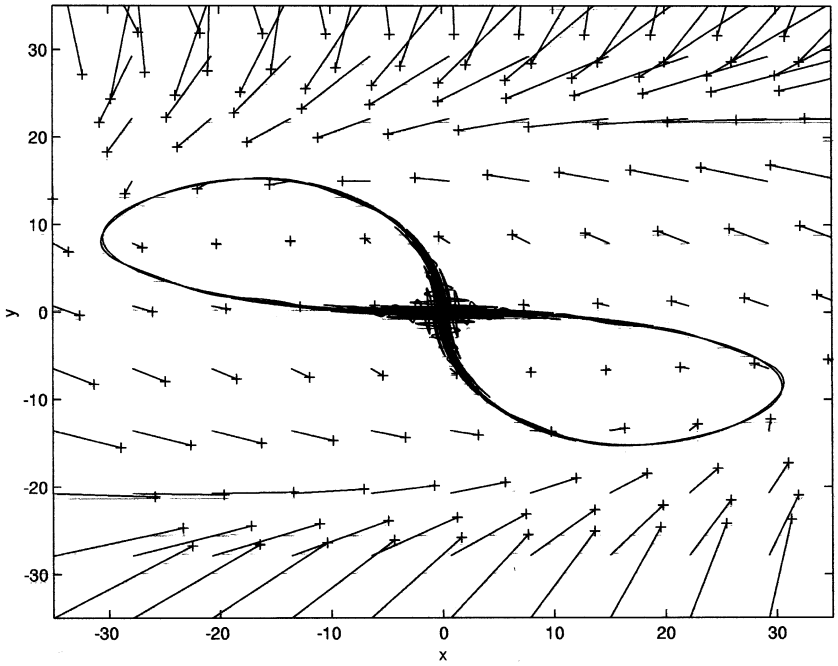

Fig. 3. A phase portrait of the stable and unstable manifolds of the map G_ε, $\varepsilon = 1/100$, in which we see a tell-tale homoclinic tangle. The phase portrait is shown on a direction-field plot of G_ε, in which direction (from tail toward "+" sign) indicates the vector change between a point and its iterate: $\lambda[G_\varepsilon(\mathbf{z}) - \mathbf{z}]$. The scaling factor λ is chosen uniformly for this figure to shorten these vectors for aesthetic reasons. We see that the rotation direction field F_ε composed with the hyperbolic saddle direction field L gives the direction field G_ε which sweeps points toward the attractor shown.

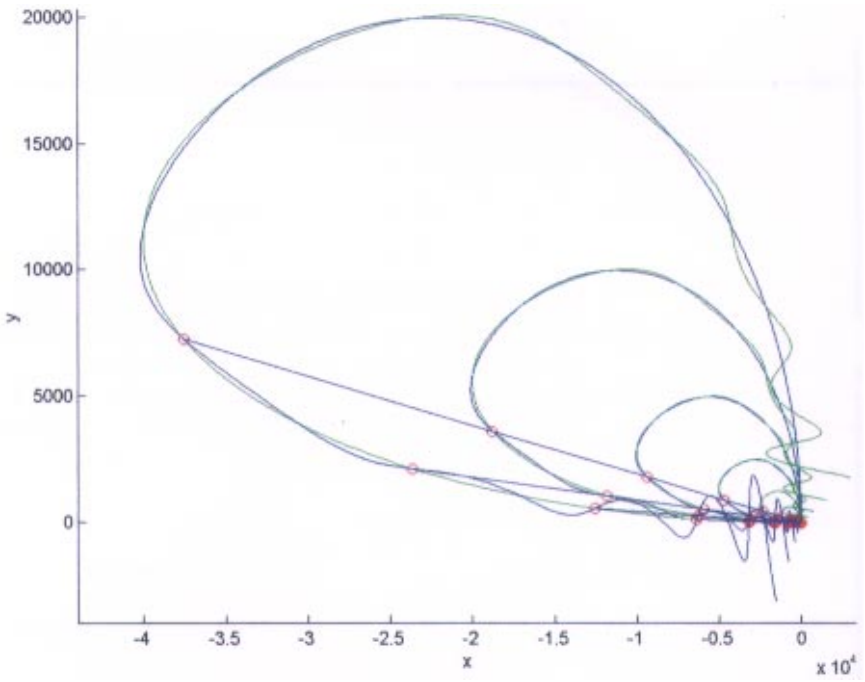

Fig. 4. A sequence of homoclinic tangles of G_{ε_i} for $\varepsilon_i = 1/2\varepsilon_{i-1}$.

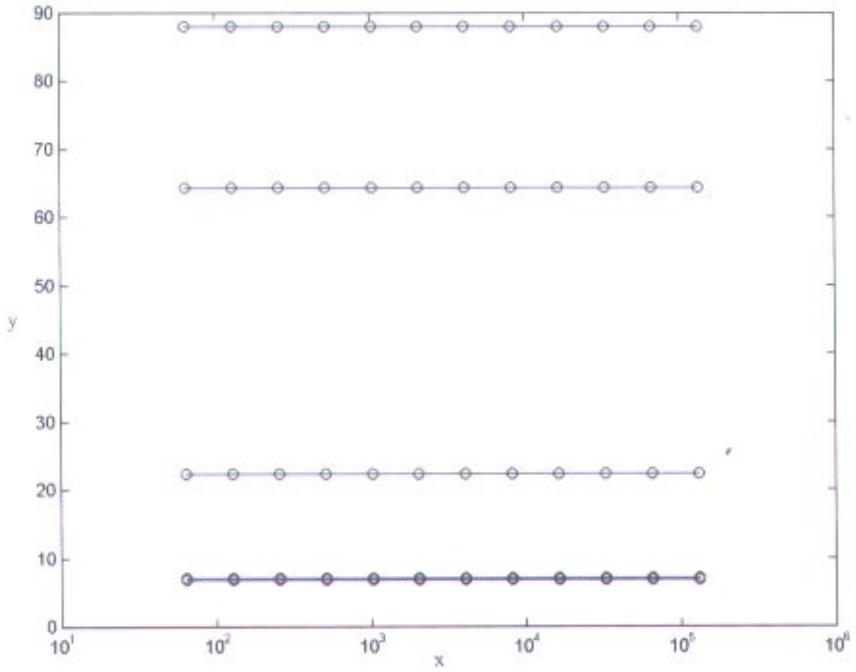

Fig. 5. Angles at transverse homoclinic points of G_ε as a function of ε. In Fig. 4, each of the highlighted sequence of primary homoclinic points shown, have angles between stable and unstable manifolds which are constant as a function of ε.

5. The Scaling Conjugacy

Adjustments to the rotation parameter ε in Eqs. (8)–(10) give the following scaling relationship,

$$G_\varepsilon(\mathbf{z}) = \frac{\tilde{\varepsilon}}{\varepsilon} G_{\tilde{\varepsilon}} \left(\frac{\varepsilon}{\tilde{\varepsilon}} \mathbf{z} \right) . \tag{12}$$

This scaling relationship is easily proven for the rotation function Eq. (10),

$$F_\varepsilon(\mathbf{z}) = \frac{\tilde{\varepsilon}}{\varepsilon} G_{\tilde{\varepsilon}} \left(\frac{\varepsilon}{\tilde{\varepsilon}} \mathbf{z} \right) , \tag{13}$$

and composition with the linear transformation L, Eq. (5), does not upset the relationship in $G_\varepsilon = F_\varepsilon \circ L$.

The implication of scaling relationship Eq. (12) is that the stable–unstable manifold structure of the fixed point $\mathbf{z} = \mathbf{0}$, for fixed ε, is geometrically similar to the stable–unstable manifold structure arising at any other $\tilde{\varepsilon}$ value. We have illustrated this fact graphically in Fig. 4, in which we see a sequence of homoclinic tangles, for a sequence of ε_i, where each $\varepsilon_i = 1/2\varepsilon_{i-1}$. From Eq. (12) follows that the homoclinic tangle doubles in size for each halving of ε, which we see in Fig. 4, and corresponding homoclinic points are connected by rays from the origin to illustrate this fact. It also obviously follows that all corresponding tangent angles of homoclinic points are preserved, see Fig. 5. Hence a transverse homoclinic point for a given fixed ε must be a transverse homoclinic point for all ε.

The above follows the fact that the scaling factor $s = (\tilde{\varepsilon}/\varepsilon)$ gives a conjugacy between $G_\varepsilon|_{\Re^2}$ and $G_{\tilde{\varepsilon}}|_{\Re^2}$ by the change of variables,

$$h(\mathbf{z}) = s\mathbf{z} , \quad s = \frac{\tilde{\varepsilon}}{\varepsilon} , \tag{14}$$

and,

$$h \circ G_\varepsilon = G_{\tilde{\varepsilon}} \circ h . \tag{15}$$

Remark 3. Any horseshoe which may exist for the map $G_\varepsilon|_{\Re^2}$ must also have a corresponding horseshoe for any other $G_{\tilde{\varepsilon}}|_{\Re^2}$. Note however, that our evidence for horseshoes for any fixed ε is numerical, following Theorem 2, by numerically finding a transverse homoclinic point as drawn in the figures. But if we believe the existence of a horseshoe for any one ε, we must believe conjugate horseshoes for all ε, by the conjugacy Eq. (15). Geometric similarity gives that even the angles of each transverse homoclinic point are preserved.

Remark 4. It follows that any ball $B_\varepsilon \subset \Re^2$ of minimal diameter d_ε, (say $\mathrm{diam}(B) = \sup_{\mathbf{z}_a,\, \mathbf{z}_b \in B} |\mathbf{z}_a - \mathbf{z}_b|$, and $d_\varepsilon = \inf_{\{B \in \Re^2 : \Lambda_\varepsilon \subset B\}} \mathrm{diam}(B)$), which contains the horsehoe set Λ_ε, must scale up to cover the horsehoe set $\Lambda_{\tilde{\varepsilon}}$ (assume $\varepsilon > \tilde{\varepsilon}$) by a factor of $1/s = \varepsilon/\tilde{\varepsilon}$, to $d_{\tilde{\varepsilon}} = d_\varepsilon/s$, as ε is reduced to $\tilde{\varepsilon}$. Thus, as $\varepsilon \to 0^+$, the diameter of a minimal covering ball must diverge, $d_\varepsilon \to \infty$.

Proposition. *$G_{\tilde{\varepsilon}}$ does not converge uniformly to L as $\varepsilon \to 0^+$.*

Proof. Following Remarks 3 and 4, we have that no compact ball can be found which covers Λ_ε for all ε. ■

Corollary. *$G_{\tilde{\varepsilon}} \to L$ pointwise, but not uniformly, as $\varepsilon \to 0^+$. This is permitted by Theorem 1.*

6. Conclusion

Thus, the seeming conflict is resolved. On the one hand, Theorem 1 says that a map "near" a map which has a horseshoe must also have a horseshoe. But "near" must be measured in terms of the uniform C^1 topology, which requires a compact domain, as discussed in remark (see footnote 2). On the other hand we have shown an example family of maps G_ε, such that each fixed ε displays a horseshoe set Λ_ε, and the family converges to a linear map, $G_\varepsilon \to L$ as $\varepsilon \to 0^+$, but the convergence is only pointwise, not uniform. The lack of uniform convergence is due to the scaling conjugacy which essentially sends points on the horseshoes Λ_ε to infinity, making impossible the definition of a single compact region to define a uniform topology. This means that Theorem 1 is of course not violated.

Hence, we have a new prototype bifurcation, which destroys/creates a horseshoe. In short, our horseshoe is sent to infinity, rather than the typical model in which it is destroyed. Typically, one thinks of the angle between stable and unstable manifolds, of a transverse homoclinic point, continuously deforming, under variations of an adjustable parameter, eventually destroying the transversality at some critical parameter value. Thus, the open neighborhood in a family of maps, promised by Theorem 1, may be realized as a single parameter path in such an adjustable parameter, as an expected interval of critical parameters. This viewpoint does not hold with our family of maps G_ε, for which angles at transverse homoclinic points must be preserved when adjusting the parameter ε.

We do in fact find that Theorem 1 applies to our family of maps G_ε, in the situation where we adjust some other parameter, such as the c or d values in the matrix L of Eq. (6) in the linear Eq. (5) built into $G_\varepsilon = F_\varepsilon \circ L$. For any fixed ε, one *can* define a compact disk to contain the horseshoe set Λ, and Theorem 1 therefore guarantees that "close-enough" functions, measured in the C^1 topology on that disk (see footnote 2), will have conjugate horseshoes. Indeed, we find that $0.4965 \approx c_{\mathrm{cr}}^- < c < c_{\mathrm{cr}}^+ \approx 0.50315$ and $1.9875 \approx d_{\mathrm{cr}}^- < d < d_{\mathrm{cr}}^+ \approx 2.014$ each give paths through these balls in function space. In Fig. 6, we show the stable and unstable manifolds of a map G_ε, $\varepsilon = 1/100$, but $c = 0.4965 \approx c_{\mathrm{cr}}$ and $d = 2$, i.e. just at the homoclinic tangency point. This displays the more traditional homoclinic bifurcation, or homoclinic tangency crisis. This is the traditional bifurcation which destroys a homoclinic point, which Theorem 1 was designed to address. Theorem 1 does apply to this situation, as we can draw a single disk, containing the family of homoclinic tangles for $c \in [c_{\mathrm{cr}}^-, c_{\mathrm{cr}}^+]$, and hence we may discuss uniform convergence.

Consequently, the type of bifurcation displayed by our map G_ε can be considered new. It is a global bifurcation in which the horseshoe is brought "from infinity" and ready-made by dialing up the adjustable parameter ε. For small values of $\varepsilon > 0$, while G_ε has a horseshoe, the chaotic nature of the dynamical system is on a slow time scale, and on a large phase space scale, that for short time intervals and small values of $\mathbf{z}_0$, the map will initially behave approximately as the linear map L.

We have also numerically observed that in Fig. 2 (lower-inset), we see that twelve iterations of the unit circle completely self-overlaps in a three-fold overlap after twelve iterations, for $\varepsilon = 1/100$, but in principle for some other number of iterations for any other ε as guaranteed by Eq. (15). This suggests the stronger statement that there is a conjugacy to a full 3-shift Σ_3, rather than simply a conjugacy to a full 2-shift as guaranteed by the horseshoe Theorem 2.

In summary, what we have proven is that by the geometric scaling conjugacy, the family of maps G_ε is topologically equivalent. Furthermore, by the fact that this conjugacy is a geometric similiarity, all relevant structures scale arbitrarily large as the control parameter is decreased $\varepsilon \to 0^+$. Hence follows the proposition that there is no

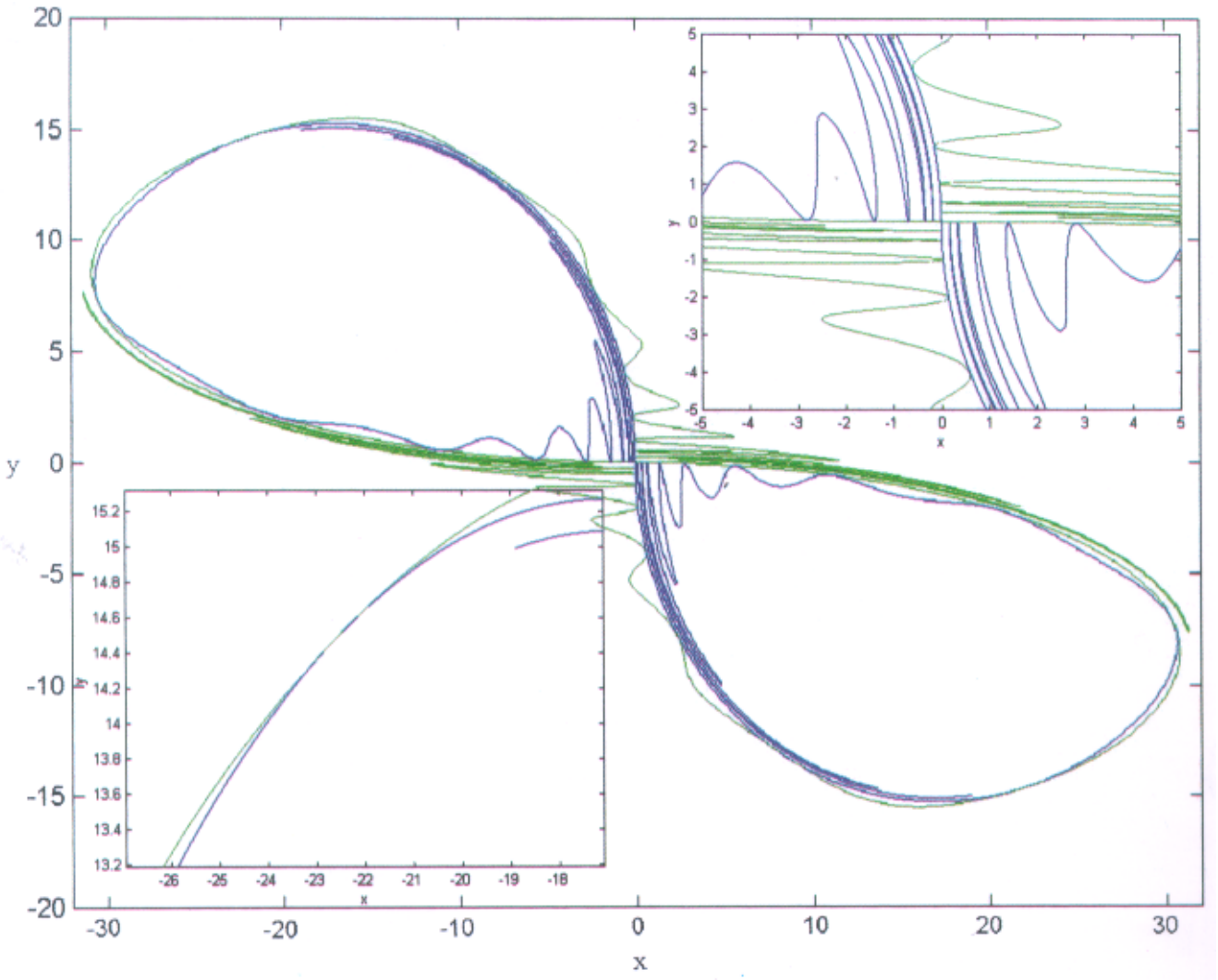

Fig. 6. A tangent homoclinic point at $c = 0.4965$. For c not in $0.4965 \approx c_{\rm cr}^{-} < c < c_{\rm cr}^{+} \approx 0.50315$, we observe no transverse homoclinic point. This is the traditional bifurcation which destroys a homoclinic point, which Theorem 1 was designed to address.

uniform convergence, and Theorem 1 does not apply. That a horseshoe exists for G_ε at any fixed $\varepsilon > 0$ follows the *numerical evidence* that stable and unstable manifolds intersect transversally. If we believe this numerical evidence, then by conjugacy we have proven that a horseshoe exists for all $\varepsilon > 0$ during the limit $\varepsilon \to 0^+$. Our future work will focus on trying to rigorously prove the existence of a transverse homoclinic point for a fixed ε.

Finally, we discuss our original motivating problem. How far is an arbitrary map from a chaotic map? We cannot answer this question in general. Instead, we offer a specific path through function space. Given an arbitrary linear map, with arbitrary matrix A, we suggest continuously deforming A to the nearest hyperbolic saddle. This can be achieved by, say, the pole-placement method [Ogata, 1990], and the distance between the given A and A' which displays a hyperbolic saddle may be measured in terms of natural matrix norms. Using the sup-norm, the matrix norm of $\|A - A'\|$ is simply the maximal absolute row sum of $A - A'$ [Golub & van Loan, 1989]. Then we proceed to define G_ε, starting from A'. This path through function space is likely not the "minimal" deformation of G_ε to $L(\mathbf{z}) = A \cdot \mathbf{z}$ distance.

Acknowledgments

I would like to thank Guanrong Chen whose talk on "anticontrol," in St. Petersburg inspired this

project. I would also like to thank Ted Stanford for helpful discussions. This work was supported by the National Science Foundation under grant DMS-9704639.

References

Bollt, E. M. & Kostelich, E. J. [1998] "Optimal targeting of chaos," *Phys. Lett.* **A245**(5), 399–406.

Bollt, E. M. & Meiss, J. D. [1995] "Targeting chaotic orbits to the moon through recurrence," *Physica* **D81**, 280–294.

Chen, G. & Dong, X. [1998] *From Chaos to Order*: *Perspectives*, *Methodologies*, *and Applications* (World Scientific, Singapore).

Chen, G. & Lai, D. [1997] "Anticontrol of chaos via feedback," *Proc. IEEE Conf. Decis. Contr.*, San Diego, CA, pp. 367–372.

Devaney, R. L. [1989] *An Introduction to Chaotic Dynamical Systems*, 2nd edition (Addison-Wesley, Redwood City, CA).

Golub, G. & van Loan, C. [1989] *Matrix Computations*, 2nd edition (Johns Hopkins University Press, Baltimore, MD).

Hirsch, M. & Smale, S. [1974] *Differential Equations*, *Dynamical Systems and Linear Algebra* (Academic Press, NY).

Kapitaniak, T. [1996] *Controlling Chaos*, *Theoretical and Practical Methods in Nonlinear Dynamics* (Academic Press Harcourt Brace and Company, Publishers NY).

Katok, A. & Hasselblatt, B. [1995] *Introduction to the Modern Theory of Dynamical Systems* (Cambridge University Press, Cambridge, UK).

Kostelich, E. J., Grebogi, C., Ott, E. & Yorke, J. A. [1993] "Higher-dimensional targeting," *Phys. Rev.* **E47**, 305–310.

Martelli, M., Dong, M. & Seph, T. [1998] "Defining chaos," *Math. Mag.* **71**(2), 112–122.

Ogata, K. [1990] *Control Engineering*, 2nd edition (Prentice-Hall, Englewood, NJ), pp. 782–784.

Ott, E. [1994] *Chaos in Dynamical Systems* (Cambridge University Press, NY).

Ott, E., Grebogi, C. & Yorke, J. A. [1990] "Contolling chaotic dynamical systems," *Chaos*: *Soviet-American Perspective on Nonlinear Science* (American Institute of Physics, NY), pp. 153–172.

Ottino, J. M. [1989] *The Kinematics of Mixing*: *Stretching*, *Chaos*, *and Transport* (Cambridge University Press, NY).

Schiff, S. J., Jerger, K., Duong, D. H., Chang, T., Spano, M. L. & Ditto, W. L. [1994] "Controlling chaos in the brain," *Nature* **370**, 615–620.

Schweizer, J. & Kennedy, M. P. [1995] *Phys. Rev.* **E52**, 4865–4876.

Shinbrot, T., Grebogi, C., Ott, E. & Yorke, J. A. [1993] "Using small perturbations to control chaos," *Nature* **363**, 411–417.

Smale, S. [1963] "Diffeomorphisms with many periodic points," in *Differential and Combinatorial Topology*, ed. Cairns, S. S. (Princeton University Press, Princeton).

Wiggins, S. [1992] *Chaotic Transport in Dynamical Systems* (Springer-Verlag, NY).